


## Formation, Structure, and Detectability of the Geminids Meteoroid Stream

W. Z. CUKIER <sup>1</sup> AND J. R. SZALAY <sup>1</sup>

<sup>1</sup>*Department of Astrophysical Sciences, Princeton University, Princeton, NJ, USA*

Submitted to PSJ

### ABSTRACT

The Geminids meteoroid stream produces one of the most intense meteor showers at Earth. It is an unusual stream in that its parent body is understood to be an asteroid, (3200) Phaethon, unlike most streams which are formed via ongoing cometary activity. Until recently, our primary understanding of this stream came from Earth-based measurements of the Geminids meteor shower. However, the Parker Solar Probe (PSP) spacecraft has transited near the core of the stream close to its perihelion and provides a new platform to better understand this unique stream. Here, we create a dynamical model of the Geminids meteoroid stream, calibrate its total density to Earth-based measurements, and compare this model to recent observations of the dust environment near the Sun by PSP. For the formation mechanisms considered, we find the core of the meteoroid stream predominantly lies interior to its parent body orbit and expect grains in the stream to be  $\gtrsim 10 \mu\text{m}$  in radius. Data-model comparisons of the location of the stream relative to Phaethon's orbit are more consistent with a catastrophic formation scenario, in contrast to cometary formation. Finally, while PSP transits very near the core of the stream, the impact rate expected by Geminids meteoroids is orders of magnitude below the impact rates observed by PSP, and hence undetectable in-situ. We similarly expect the upcoming DESTINY+ mission to be unable to detect appreciable quantities of Geminids grains far from (3200) Phaethon.

### 1. INTRODUCTION

Meteoroid streams provide a discrete view into the dynamics and evolution of material in the zodiacal dust cloud. Much of our knowledge of meteoroid streams comes from Earth-based observations, where meteoroids ablate in the atmosphere and produce meteor showers observable via visual or radar-based systems. These detections rely on the Earth directly intersecting a substantial portion of the meteoroid stream and likely there are many streams in the solar system we do yet know of.

In this study, we focus on the Geminids meteoroid stream. It is an unusual stream as it is one of the strongest streams observed at Earth (e.g. Jenniskens 1994) and is associated with asteroid (3200) Phaethon, instead of the typical cometary parent body of most streams. It has also been associated with asteroids 2005 UD and 1999 YC (e.g. Jewitt & Hsieh 2006), which may provide evidence of all 3 bodies being formed from a catastrophic breakup of an initial comet parent body. The first well-documented observation of the Geminids occurred in 1862 (Greg 1872; King 1926) and has been studied considerably in the last half-century, both via observations (e.g. Jenniskens 1994; Arlt & Rendtel 2006; Brown et al. 2008; Jewitt & Li 2010; Li & Jewitt 2013) and from a theoretical/modeling framework (e.g. Fox et al. 1982, 1983; Ryabova 2007, 2008, 2016, 2017, 2021; Williams & Ryabova 2011). Many reviews of this shower have also been undertaken in the literature (e.g. Zigo et al. 2009; Neslušan 2015; Jakubík & Neslušan 2015; Hajduková Jr et al. 2017).

The Parker Solar Probe (PSP) spacecraft, launched in orbit about the Sun in 2018 (Fox et al. 2016) is exploring the inner-most regions of our solar system's zodiacal dust cloud. PSP's WISPR imager has made direct high-resolution

visual images of the Geminids meteoroid stream very near to the Sun (Battams et al. 2020) and discovered the core observable stream is offset radially outward from (3200) Phaethon’s orbit. Additionally, PSP can directly observe its very local dust environment (Battams et al. 2022). While it does not have a dedicated dust detector, it is able to detect the total impact rate of dust grains to the surface of the spacecraft on the FIELDS instrument (Bale et al. 2016) via transient spacecraft potential changes due to the impact plasma from high-velocity impactors. The first few orbits of data were dominated by impacts from  $\beta$ -meteoroids (Szalay et al. 2020), fragments so small they are expelled from the solar system on unbound orbits due to radiation pressure. The peak fluxes of these grains were found to vary by  $\sim 50\%$  over the first three orbits (Malaspina et al. 2020). Analysis of the directionality of impactors over the first few orbits also indicated the possibility of bound  $\alpha$ -meteoroids and retrograde impactors (Page et al. 2020). After PSP’s initial orbit was successively lowered by flybys with Venus, comparison with a two-component model for the zodiacal cloud found its impact rates in subsequent orbits contained appreciable amounts of both  $\alpha$ -meteoroids and  $\beta$ -meteoroids (Szalay et al. 2021). A third source of impactors was identified that was not attributable to the nominal zodiacal cloud and was suggested to be either due to direct observations of meteoroid streams or their collisional byproducts in the form of a concentrated stream of  $\beta$ -meteoroids, a  $\beta$ -stream (Szalay et al. 2021). Broad estimates for the  $\beta$ -stream fluxes and analysis of the directionality of impactors (Pusack et al. 2021) both favored a  $\beta$ -stream source over direct observations of meteoroid streams, but the exact origins of this third impactor source remain unresolved.

While direct observations of meteoroid streams have been inferred by Helios data (Krüger et al. 2020), the densities required for such an observation and for PSP (Szalay et al. 2021) are on the order of  $10\text{--}100\text{ km}^{-3}$ . Here, we create a dynamical model of the Geminids with three simplified formation mechanisms to test if the Geminids meteoroid stream could be directly detectable by PSP and explain the unresolved third impactor source. We also investigate the structure of the stream and how it is dependent on the specific formation mechanism, specifically in comparison to PSP’s remote observations showing the stream lies outside its parent body orbit (Battams et al. 2022). In Section 2 we describe the dynamical model. We compare the model to Earth-based and PSP observations in Section 3 and conclude with a discussion on implications and implications of model assumptions in Section 4.

## 2. SIMULATION METHODOLOGY

The mass of the Geminids stream is estimated to be on the order of or larger than the parent body (3200) Phaethon (Blaauw 2017; Ryabova 2017), which suggests it was formed in a possibly catastrophic event that shed a large amount of mass in a relatively short period of time approximately 2000 years ago (Fox et al. 1983; Ryabova 1999). A rapid cometary hypothesis has been shown to reproduce aspects of the Earth-based observations of the Geminids (Ryabova 2021). While there is cometary-like activity currently occurring at (3200) Phaethon, the mass loss from this activity is orders of magnitude too low to sustain the Geminids (Jewitt & Li 2010; Jewitt et al. 2013, 2018; Tabeshian et al. 2019). Additionally, (3200) Phaethon will also experience an intense impact environment from co-orbiting dust in the zodiacal cloud near each perihelion, which ejects sub-micron to mm-sized material from the surface as well, but this mechanism is only estimated to be produce  $10^5 - 10^6$  kg of ejecta over 2000 years (Szalay et al. 2019), orders of magnitude too little material to appreciably contribute to the stream mass of  $10^{13} - 10^{15}$  kg (Blaauw 2017; Ryabova 2017). Electrostatic dust ejection has been proposed as a mechanism for the observed activity of (3200) Phaethon and possibly also as a source for the entirety of the Geminids stream (Kimura et al. 2022). Here, we simulate the formation of the stream as a catastrophic event occurring 2000 years ago and do not consider the effects of an ongoing source from (3200) Phaethon.

We consider three simplified creation scenarios for the Geminids stream: a) all the particles were released at (3200) Phaethon perihelion at velocity of 0 relative to the parent body as a basic model for a basis of comparison, b) all the particles were released at (3200) Phaethon perihelion with a velocity dispersion on the order of 1 km/s relative to the parent body to simulate a violent creation event and c) an elementary cometary model where the particles are released throughout a single orbit of (3200) Phaethon at a rate inversely proportional to the distance from (3200) Phaethon and the Sun.

### 2.1. Basic Model

We simulated 10,000 particles for each of the Basic Model and the Violent Creation Model. These particles were released from perihelion at the same location and velocity as (3200) Phaethon 2000 years ago. Given the particles were released at perihelion, only  $\beta$ -values low enough that particle escape would not happen needed to be simulated. Following Burns et al. (Eq. 23, 1979), grains released from perihelion with  $\beta \geq (1 - e)/2$  are unbound and travel

in hyperbolic orbits. The maximum  $\beta$ -value that need be considered for particles released from (3200) Phaethon at perihelion is  $\beta = 0.052$ , which for the “asteroidal” model from Wilck & Mann (1996) with particle density of  $\rho = 3205$  kg/m<sup>3</sup>, corresponds to particles with a mass of  $2.4 \times 10^{-9}$  g and radius of 12  $\mu$ m. For the Basic Model, the 10,000 particles were chosen to be evenly distributed in  $\beta$ -space from  $\beta = 0$  to  $\beta = 0.052$ .

The simulation was run from (3200) Phaethon perihelion on Jan 2, 19 A.D. for 2000 years using **Rebound** N-body code (Rein & Liu 2012). The simulations were integrated using IAS15, a 15th order Gauss-Radau integrator (Rein & Spiegel 2015). Ephemeris of (3200) Phaethon from 1600 A.D. was taken from JPL HORIZONS and back-integrated to the start date. In this scenario, particles were released at perihelion with the same state vector as (3200) Phaethon.

For each model, **Reboundx** (Tamayo et al. 2020) was utilized to calculate the forces of radiation pressure and Poynting-Robertson drag. Gravitational forces from the Sun, 4 inner planets, and Jupiter were considered in the simulation, data for which was taken from NAIF SPICE kernels (Folkner et al. 2014). We used only 5 instead of a full 8 planets to save on computational time. A test run of the basic model with all 8 planets caused only minor changes—a slight antisunward shift in the stream at perihelion and a change in the predicted stream mass that was significantly smaller than other uncertainties. Dust particles were treated as test-particles that do not interact with each other. For some configurations of parameter space, some particles would either get ejected from the solar system or become unphysically close to the Sun where they would breakup via collisions or sublimation (e.g. Mann et al. 2004). Here, we do not include the effects of sublimation/collisions and instead remove grains with very small semi-major axes from our simulation. Particles with a semi-major axis of 0.2 au or below were removed from the simulation under the assumption that their interactions would be dominated by zodiacal collisions, sublimation and/or sputtering very near to the Sun. Additionally, particles that during any time step were less than 0.01 au or greater than 10 au from the Sun were removed from the simulation due to numerical concerns. For each of the first 1998 years of the simulation the semi-major axis, eccentricity, inclination, argument of perihelion, and longitude of ascending node were stored for each particle.

During the last two years of the simulation, the position vector for each particle was stored at 2000 instances equally spaced in time. Each of these snapshots was then treated as a separate particle for the remainder of the analysis. Particles were then weighted according to a mass power law as follows:  $\beta$ -mass relations were taken from Wilck & Mann (Fig. 2, 1996), treating the grain compositions as typically asteroidal, and extrapolated using a power law fit to the descending half of the curve (from  $\sim 10^{-13}$  g to  $\sim 10^{-8}$  g).

The differential mass distribution for the Geminids stream is assumed to follow a power-law,

$$f(m) \propto m^{-s} \quad (1)$$

where  $s$  is taken to be  $1.68 \pm 0.04$  (Blaauw 2017). Integrating this differential mass distribution from a minimum mass,  $m_0$ , to  $m$  the cumulative mass distribution for the stream can be modeled as:

$$F(m) = \frac{m^{1-s} - m_0^{1-s}}{m_1^{1-s} - m_0^{1-s}} \quad (2)$$

where  $m_0$  was  $10^{-9}$  g, below which particles released at perihelion would be ejected from the solar system and the maximum mass,  $m_1$  was chosen to be 10 g.

Particles were then weighted by first converting the 10,000  $\beta$ -values into mass values as described above and then determining the mass range each particle represents by subtracting the cumulative mass of the particle with the next smallest mass from the cumulative mass of the current particle. Each particle was then given a weight in the model equal this the amount of cumulative mass space the particle represents.

## 2.2. Violent Creation Model

While the “Basic” model described in the previous section provides a basic framework to simulate a catastrophic event, we also investigate the effect of the speed distribution of source particles to provide a more realistic scenario for a “Violent Creation” of the Geminids. To model a this violent creation event, the particles were released with a speed distribution that has a maximum speed on the order of 1 km/s relative to the parent body. Most of the implementation details for this Violent Creation Model are the same as for the Basic Model with the exception of the additional particle velocity and that the 10,000 simulated particles were now only split among 100  $\beta$ -values instead of each particle having a unique  $\beta$ -value.

To simulate a more violent creation mechanism, we initialize particles with an isotropic angular distribution with respect to their parent body. We use a statistical sampling process to create this isotropic velocity distribution where we determine the direction of the velocity vector for each individual particle by sampling points randomly within a unit cube and rejecting points that lied outside the unit sphere. After this procedure, we have a set of isotropically distributed unit vectors representing the additional velocity boost particles gained by the violent creation event. We then determine the absolute speeds of each particle following Durda (1996), described below. This provides an experimentally-driven model for the expected velocity distribution. We note that it is not possible to directly replicate asteroidal breakup conditions in the laboratory setting and must assume the relation used here scales to our specifically simulated regime. The “typical” ejection speed  $V_a$  for a particle with mass  $m$  was determined using the power law:

$$V_a = C m^{-r} \quad (3)$$

where  $C = 0.182 \text{ m/s/g}^{0.1}$  was picked such that the average (un-weighted) typical speed of the simulated particles was scaled to  $\sim 1 \text{ km/s}$  and where  $r = 0.1$ . A random scale factor,  $x$  was then chosen uniformly between 0 and 4. A second random number,  $y$  uniformly chosen between 0 and 1 was then compared with the Maxwellian function:

$$(x^2 e^{-x^2+1})^w \quad (4)$$

where  $w$  was picked to equal 1. If that second random number,  $y$  was less than the Maxwellian function, then the particle is assigned the velocity  $V = xV_a$ , otherwise  $x$  was rechosen.

Unlike in the Basic Model, only 100  $\beta$ -values were evenly chosen between  $\beta = 0$  and  $\beta = .052$ . At each of these  $\beta$ -values, 100 particles were simulated, each with separately chosen velocities.

### 2.3. Cometary Model

For the Cometary Model, particles were released at locations throughout a single orbit of (3200) Phaethon 2000 years ago. Due to the increased complexity of this simulation and the frequency at which particles escaped or spiraled into the Sun, the number of particles simulated was increased to 100,000 for this model. Particles were released at 100 locations, 50 on either side of perihelion, equally spaced in their radial distance from the Sun. At each location, the maximum theoretical  $\beta$ -value for bound particles was determined and 1000 particles were released at a relative velocity of 0 m/s relative to (3200) Phaethon, evenly spaced in  $\beta$ -space. The model weight,  $w$ , is assigned to each particle as follows:

$$w = \frac{Mt}{r^4} \quad (5)$$

where  $M$  is the amount of cumulative mass space represented by the particle, similar to the weighting functions of the Basic Model and Violent Creation Model,  $r$  is the distance between the particle location and the Sun and is to the  $-4$  power following Ryabova (2007), and  $t$  represents the amount of time (3200) Phaethon spent closest to this release location as opposed to one of the other 99 modeled release locations.

## 3. RESULTS

### 3.1. Stream Characteristics

Column densities of the modeled streams in the Ecliptic J2000 frame during the last two years of simulation are presented in Figure 1. Note these show column density, not 3D density, and thus represent the number of particles per area along a particular line of sight. To demonstrate how the particle size varies throughout the stream we additionally plot column densities for extremely small particles ( $m < 10^{-7} \text{ g}$ ) and large particles ( $m > 10^{-5} \text{ g}$ ) in Figure 2. We also present plots of the “unwrapped” stream in Figure 3. These quantities were generated by projecting the particles to the orbit of (3200) Phaethon and then calculating the distance from the particle to that point against the arc length distance of that point from perihelion.

The Basic Model has a relatively dense central core to the inside of the the orbit of (3200) Phaethon and a less dense outer stream composed of lighter particles that is outside the orbit of (3200) Phaethon. As expected, particles that orbit near the orbit of (3200) Phaethon are generally the most massive and the mass of particles decreases further inwards from the orbit of the parent body. There additionally appears to be a secondary stream outside of the orbit of (3200) Phaethon composed of extremely small particles at a larger radius. Particles with  $\beta < 0.02$  generally were dominated by Poynting-Robertson drag and had a final orbit inside that of (3200) Phaethon while those particles with

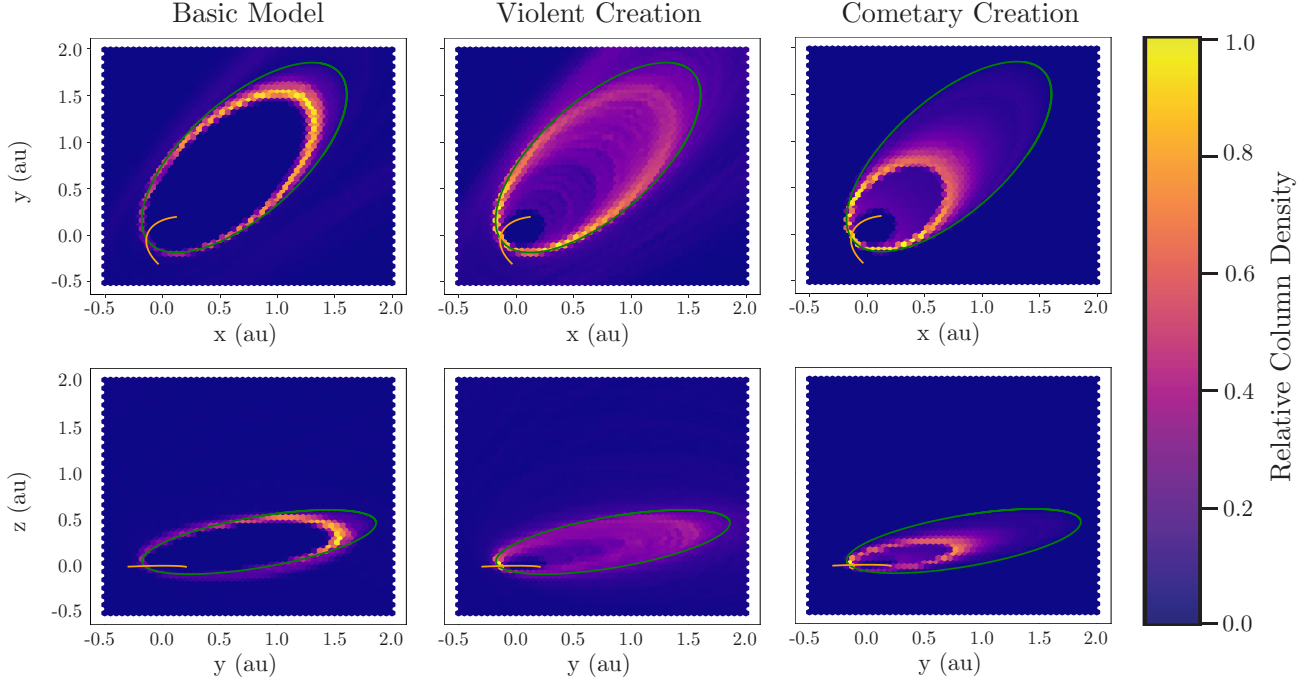


**Figure 1.** Number column density of the Geminids stream in the x-y (top) and y-z (bottom) planes as described by the basic model (left) and Violent Creation Model (mid), and Cometary Creation Models (right) during the last two years of simulation. Densities are normalized to 1 in each panel independently. The green ellipse is the orbit of (3200) Phaethon, the orange curve is the orbit of PSP during the anomalous spike in dust flux. All panels are in Ecliptic J2000 coordinates. Note that particles with a semi-major axis of  $a < 0.2$  were removed from the simulations leading to the discontinuity in density near the Sun in the Cometary Creation Model.

$\beta > 0.02$  were boosted to large enough orbits by radiation pressure that after the 2000 year simulation they still had orbits larger than that of (3200) Phaethon, leading to the development of a secondary stream. The fact that this secondary stream is composed primarily of light particles, however, means that this stream only accounts for about 0.07% of the total mass of the stream.

The Violent Creation Model yields a more dispersed stream than the Basic Model due to the initial additional velocity spread for the grains. The densest part of the stream occurs near perihelion as most particle spread happens near aphelion. As seen in Figure 2, this model leads to a relatively more homogeneous distribution of particle size throughout the stream compared to the Basic Model, likely due to the mixing caused by the initial speeds given to each particle at the start of the simulation. The average final semi-major axis of a particle at a given value for  $\beta$  follows the same trend as for the Basic Model but the variation within each  $\beta$ -bin is far greater than the variation between  $\beta$ -bins, especially for  $\beta < 0.02$ .

The Cometary Creation Model yields a stream in which most of the particles orbit inside the orbit of (3200) Phaethon. This is likely due to the fact particles released at further distances from the Sun will experience a smaller boost in initial semi-major axis due to radiation pressure so the effects of Poynting-Robertson Drag will more easily dominate. This effect is most pronounced for small particles which have larger Poynting-Robertson Drag and thus shorter decay timescales. When running the simulations of this model, we noticed that before weighting,  $\sim 85\%$  of the surviving particles after 2000 years had a  $\beta < 0.05$ . There was a small cluster of remaining particles at  $\beta = 0.3$  and the rest were about evenly distributed over the  $\beta$ -range. To increase the resolution of the model and to focus more on detectable particles, we reran the simulation with a maximum  $\beta$ -value of 0.05, corresponding with a minimum mass of  $2.8 \times 10^{-9}$  g. We use the results of this  $\beta < 0.05$  limited simulation instead of the full  $\beta$ -range in all of our analysis and figures.

The key difference between the models is the Basic Model expects a well-defined stream just inside the orbit of (3200) Phaethon, the Violent Creation Model expects a more dispersed stream but still centered on the same orbit as the Basic Model, and the Cometary Creation model predicts a stream that has decayed significantly and, while spread out, has a stream core, which we define as the region with the greatest particle density, with a semi-major axis  $a < 1$  AU.

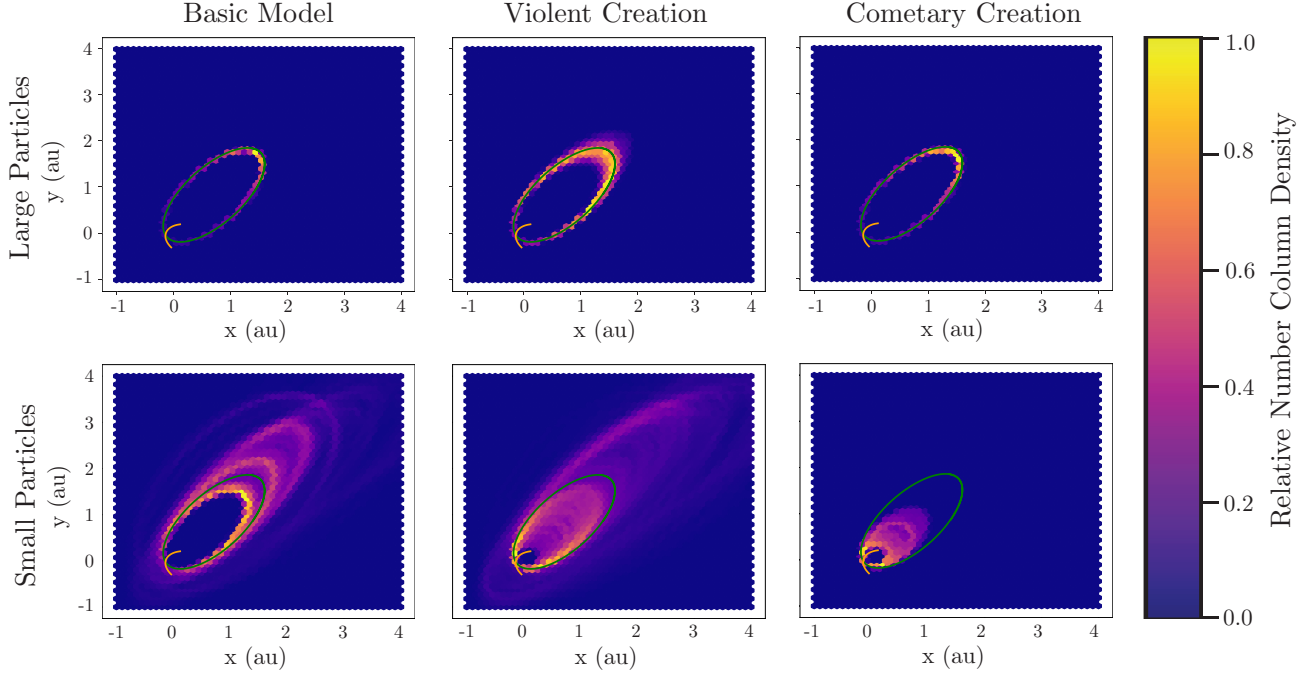


**Figure 2.** Number column density of the Geminids stream in the x-y plane as described by the Basic Model (left) and Violent Creation Model (mid), and Cometary Creation Model (right) during the last two years of simulation. Densities are normalized to 1 in each panel independently. The green ellipse is the orbit of (3200) Phaethon, the orange curve is the orbit of PSP during the anomalous spike in dust flux. All panels are in Ecliptic J2000 coordinates. Note that particles with a semi-major axis of  $a < 0.2$  were removed from the simulations leading to the discontinuity in density near the Sun in the Cometary Creation Model. The top panels show “large particles” which are defined as particles with  $m > 10^{-5}$  g, which are the particles that we consider at Earth in Section 3.2. The bottom panels show “small particles” which are defined as particles with  $m < 10^{-7}$  g.

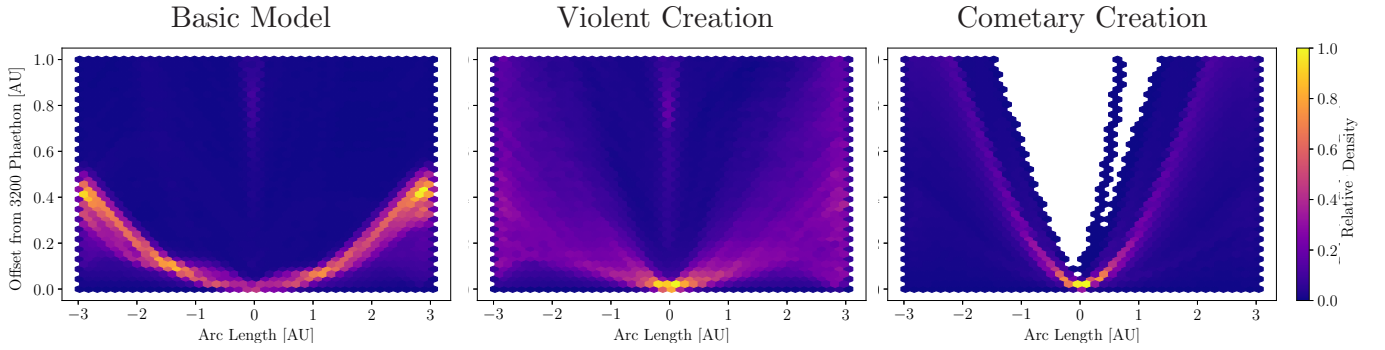


**Figure 3.** The relative number of particles located at each point around the “unwrapped” orbit of (3200) Phaethon for the Basic Model (left) Violent Creation Model (middle) and the Cometary Creation Model (right) during the last two years of simulation. To create this figure each particle was radially projected onto the orbit of (3200) Phaethon and then the distance between that point and the particle was calculated. The white area in the rightmost panel is locations where no particles exist and is caused by some combination of the removal of particles that are too close to the sun and the fact that little to no particles exist outside the orbit of (3200) Phaethon in the Cometary Model.

We additionally present the evolution of orbital elements of the stream over time in Figure 4. These were made by taking the average of the orbital elements for each surviving particle with mass  $m > 1 \times 10^{-8}$  g, weighted by the model weights described above, for each year during the simulation. This limiting mass is applied to limit our analysis to the primary stream. Clearly demonstrated in these plots is the effect of Poynting-Robertson drag circularizing the orbits of the streams as seen by the average semi-major axis and eccentricity for all three models being driven down over time. Note that for the Cometary Creation Model in particular, the change in eccentricity appears to be accelerating. The differing initial semi-major axis and eccentricities for the Basic Model and Violent Creation Model is

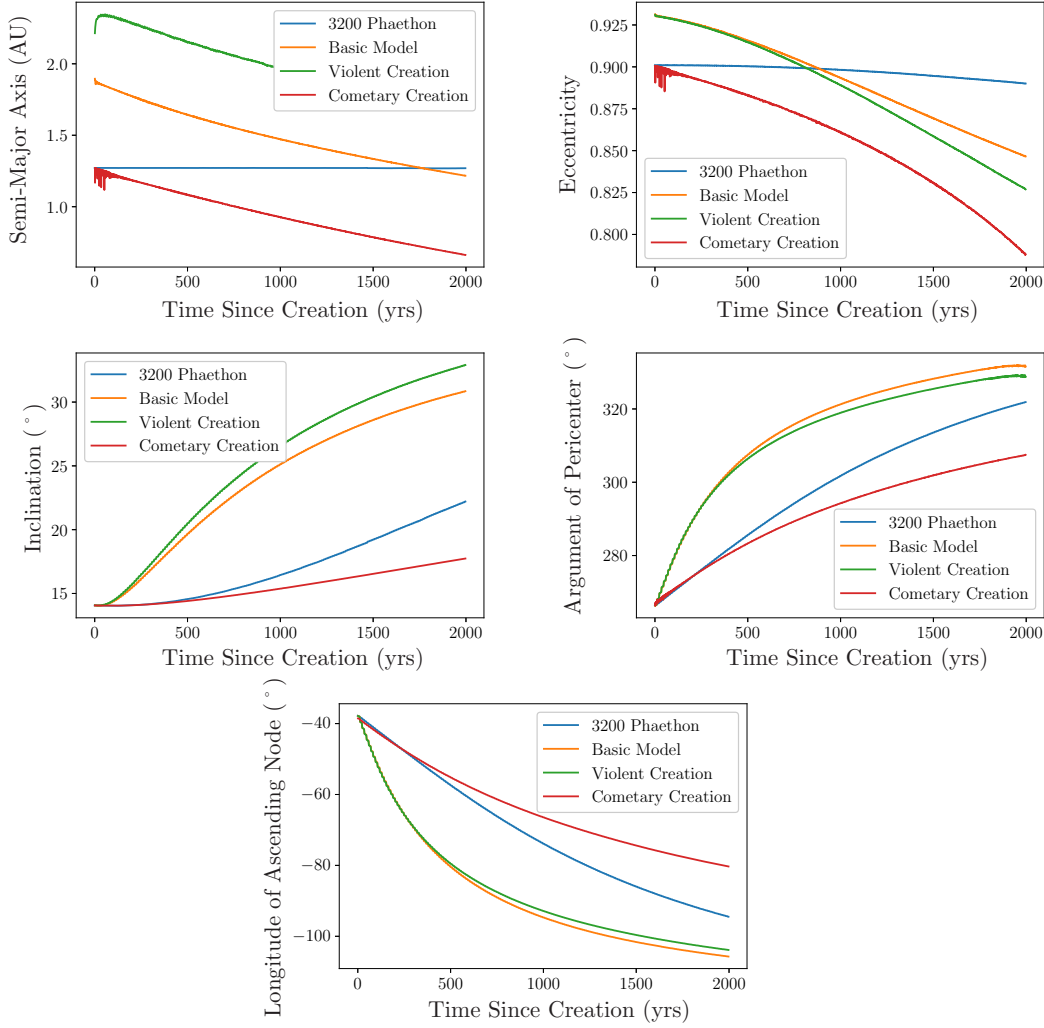


**Figure 4.** Time evolution of the orbital elements of the average particle in the primary stream ( $m > 10^{-8}$  g) from the model variants and for (3200) Phaethon. All elements are measured in the Ecliptic J2000 frame. Top Left: Semi-Major axis. Top Right: Eccentricity. Middle Left: Inclination ( $^{\circ}$ ). Middle Right: Argument of Pericenter ( $^{\circ}$ ). Bottom: Longitude of Ascending Node ( $^{\circ}$ ).

caused by the radiative forces being suddenly turned on at perihelion, as is done in our models, causing an immediate shift the aphelion positions of the particles. This effect is not seen in the Cometary Creation Model because the instantaneous effect of radiative forces is not as significant for particles released further away from the Sun. We also note that the Cometary Creation Model exhibits slower precession than (3200) Phaethon while the Basic Model and Violent Creation Models exhibit faster precession than their parent body. An additional effect likely demonstrated by the model is the Kozai-Lidov mechanism where the reduction in eccentricity leads to an increase in the inclination of the model (Kozai 1962).

### 3.2. Geminids Stream at Earth

To normalize the model results to real physical units, we compare with Earth-based observations of the Geminids stream. To do so, we calculate the density of meteoroids in a 0.03 AU sphere centered on Earth at each of 8000 points along its orbit. Note that the selection of sphere radius does add uncertainty to the stream mass and timing and can substantially alter the full-width, half-maximum of the stream. We chose a .03 AU sphere as the Basic Model and Cometary Creation Model do not register more than a couple particles for a .02 AU sphere. We then calculate the flux incident on Earth by treating Earth as a flat plate detector perpendicular to the stream of meteoroids that are

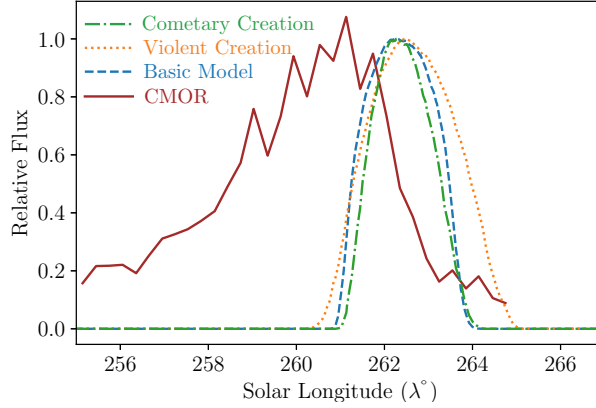


**Figure 5.** Plot of the normalized impactor flux upon Earth as predicted during the last two years of simulation by the Basic Model (blue dashed line), the Violent Creation Model (orange dotted line) and Cometary Creation Model (green dot-dashed line) compared to observational data taken from CMOR (solid red line) (Jones et al. 2005).

Model	Mass (g)	Peak Time ( $\lambda^\circ$ )	Full-Width, Half-Max ( $\lambda^\circ$ )	Closest Approach (au)
Basic	$4.7(\pm 3.7) \times 10^{14}$	262.26	2.34	0.019
Violent	$6.3(\pm 3.7) \times 10^{13}$	262.51	2.79	0.0017
Cometary	$8.6(\pm 4.3) \times 10^{14}$	262.14	1.97	0.017

**Table 1.** Predicted and derived physical characteristics of the stream at Earth for each of the models. The peak flux observed by CMOR occurs at  $\sim 261.1^\circ$ . The error in Geminids mass was calculated by propagating the error in CMOR flux and the Geminids power law index taken from Blaauw (2017).

incident upon it at 35 km/s. The normalized flux is compared to that of CMOR as shown in Figure 5. The minimal limiting mass for the meteoroids is taken to be  $1 \times 10^{-5}$  g whereas the limiting mass for CMOR is  $1.8 \times 10^{-4}$  g following Blaauw (2017). The lower mass limit allows the Cometary Creation Model to be detected at Earth as no particles from the Cometary Creation Model with mass above  $1.8 \times 10^{-4}$  g were detected within 0.05 AU of Earth. This lower limiting mass will cause the stream mass to be underestimated and the peak time to be slightly earlier. We note there are multiple other observations of the Geminids at Earth (e.g. Kero et al. 2013) and the Moon (e.g. Szalay et al. 2018), however, we limit the comparison to CMOR as a nominal example of the profile and as these measurements were used to derive the total stream mass.

The stream mass for each model is estimated by scaling up the peak meteoroid flux observed at Earth to the peak flux observed by CMOR as follows:

$$M_{\text{geminids}} = M_{\text{model}} * \frac{F_{\text{CMOR}}}{F_{\text{model}}} * \frac{m_{\text{model limit}}^{1-s} - m_{\text{max}}^{1-s}}{m_{\text{CMOR limit}}^{1-s}} \quad (6)$$

where  $M_{\text{model}}$  is the weighted sum of the mass of the 10,000 particles used in the model,  $F_{\text{model}}$  is the weighted particle flux upon Earth as predicted by the model,  $F_{\text{CMOR}} = 6.64 \times 10^{-2}$  meteors /km<sup>2</sup>/hr– which was determined by scaling the off-peak flux given in Blaauw (2017) to the time of peak flux,  $m_{\text{max}} = 10$  g is the maximum mass considered by the model,  $m_{\text{CMOR limit}}$  and  $m_{\text{model limit}}$  are the limiting values for CMOR and the model respectively as discussed above, and  $s = 1.68$  is the mass power law we have used throughout this paper. The last fractional part of this equation is derived from Equation 2 and used to account for the fact that our model theoretically registers a greater fraction of the Geminids meteoroids than CMOR due to the lower limiting mass. The masses estimated by this model range from  $6.3 \times 10^{13}$  g for the Violent Creation Model to  $8.6 \times 10^{14}$  g for the Cometary Creation Model. These values are about one half to one order of magnitude smaller than the other estimates of the mass of the Geminids stream when adjusted for the limiting mass ranges of previous estimates (Ryabova 2017; Blaauw 2017). A comparison of each model at Earth with observational CMOR data is visible in Figure 5. A summary of physical characteristics of the stream at Earth is visible in Table 1.

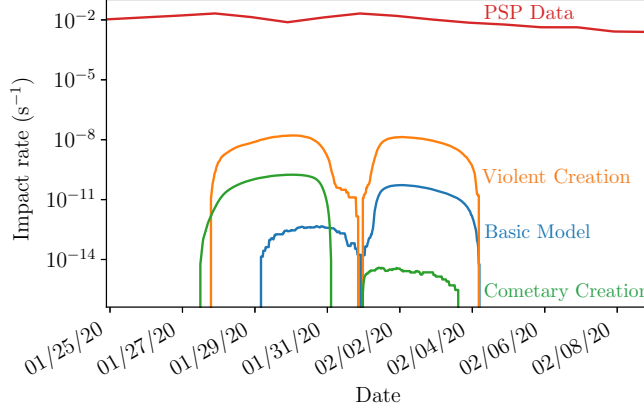


**Figure 6.** Dust flux incident on the Parker Solar Probe from the Geminids stream around perihelion of orbit 4 of PSP as predicted during the last two years of simulation by the various models and compared with the observed dust flux showing the post perihelion enhancement. Dust flux was modeled using the density of meteoroids within 0.05 au of PSP. PSP impact rates are from previously published observations (Szalay et al. 2021).

Model	a	b	c
Basic	$-91 \pm 15$	$1.4(\pm 0.7) \times 10^3$	$4.3(\pm 0.6) \times 10^5$
Violent Creation	$34 \pm 22$	$-400 \pm 1100$	$-1.3(\pm 0.9) \times 10^5$
Cometary Creation	$-270 \pm 10$	$-7.9(\pm 0.6) \times 10^3$	$-1.6(\pm 0.5) \times 10^6$

**Table 2.** Coefficients of the fitted parabola  $y = ax^2 + bx + c$  where  $x$  is the mean anomaly in degrees and  $y$  is the signed offset from the orbit of (3200) Phaethon of the core of the meteoroid stream. These fits are shown in Figure 7.

The flux at Earth for each of these models peaks at approximately  $262.2^\circ$  for each of the models. While this is in agreement with the traditional visual peak of the Geminids at  $262.2^\circ$ , it disagrees with CMOR observations by about  $0.9 - 1.3$  days dependent on model as CMOR peaks at about  $261.4^\circ$ . CMOR observes meteors with magnitudes down to  $+8$ , which are fainter than the more massive and therefore brighter and human-eye visible meteors that peak later. Given the models' limiting masses are designed to mimic CMOR's detection limit, the likeliest explanation is model uncertainty with respect to precise formation mechanism.

A key thing to note is that none of the models were able to have any particles collide with Earth—the Violent Creation Model had a closest approach distance of .0024 AU while the Basic Model and Cometary Creation Model had closest approaches on the order of 0.02 AU. Given that only 10,000 or 100,000 particles were simulated dependent on model, this fact is likely in part due to low sample sizes, particularly for the Violent Creation Model. We also only consider 1000 points in space for each particle over a two year orbit which impacts the spacial resolution data. Notably, the meteoroids from the Violent Creation Model had a closest approach to Earth an order of magnitude closer than the other models, likely due to the randomness included in the Violent Creation Model allowing for more particles to closely approach Earth. This inability to exactly model the impact at Earth has been exhibited by other models in the literature (Ryabova 2007, 2017) which likely indicates a not yet fully understood or postulated mechanism.

### 3.3. Space Missions

#### 3.3.1. Parker Solar Probe

Similar to how the flux at Earth was calculated, the flux incident on the Parker Solar Probe was estimated by determining the density of dust particles within 0.05 AU of PSP at each of 8000 points along PSP's orbit and then calculating how many particles PSP would hit if it flew through a cloud of particles at that density. To achieve an upper bound on that calculation we assumed PSP was a flat plate dust detector facing perpendicular to every particle and moving at a speed relative to the particles equal to the sum of the orbital speed of PSP with respect to the Sun and the speed of (3200) Phaethon at perihelion. The total mass of the stream for this calculation was set to  $10^{14}$  g. We additionally assume that every particle, regardless of mass, registers on PSP with 100% efficiency. Using these

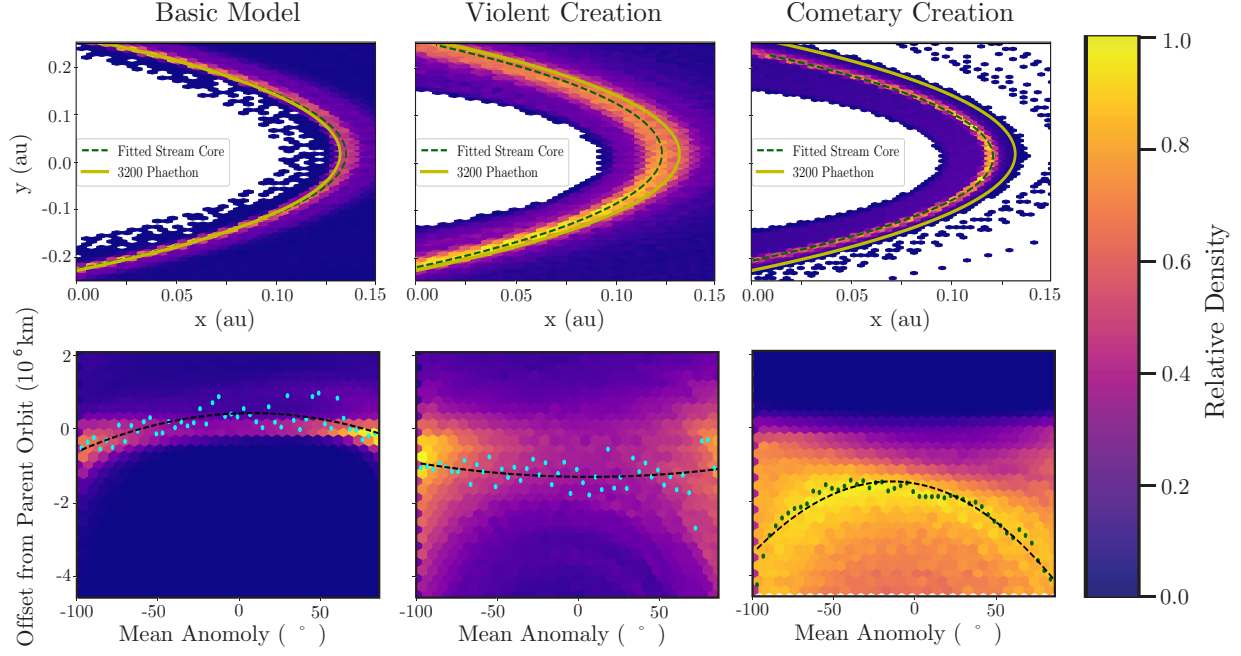


**Figure 7.** Top: Number column Density plots in the plane of the orbit of (3200) Phaethon for the Basic Model (left) Violent Creation Model (mid) and the Cometary Creation Model (right) during the last two years of simulation. Shown over top these plots is the orbit of (3200) Phaethon (yellow solid line) and the fitted core of the modeled stream (dashed green line). Bottom: The relative number of particles at each signed offset from the orbit of (3200) Phaethon as a function of mean anomaly. Cyan and dark green points in the bottom panel show the center of the radial bins of maximum density for each mean anomaly bin. The dashed line is a parabolic fit to those points and is taken to represent the core of the stream. Coefficients of the parabolic fit can be found in Table 2.

assumptions we find that the impact rate was on the order of  $10^{-8} \text{ s}^{-1}$  for the Violent Creation Model and on the order of  $10^{-9} - 10^{-11}$  for the Basic Model and Cometary Creation Model, meaning that our models of the Geminids do not provide sufficient impact rates to explain the post perihelion rate enhancement observed by PSP (Szalay et al. 2021). The predicted impact rate due to the Geminids stream to PSP is shown in Figure 6. This figure also shows in-situ impact rate data from PSP’s orbit 4, as a representative orbit where the second peak is attributed to a possible Geminids-related source (Szalay et al. 2021).

We additionally present a more detailed prediction of stream observations near perihelion. We present in Figure 7 column densities in the plane of the orbit of (3200) Phaethon along with a fitted “core” of the stream. Additionally shown is the plane-projected offset of the stream from Phaethon’s orbit as a function of the mean anomaly. Fitting the core of a point cloud is an imprecise task. To do so we first binned the particles by mean anomaly. These bins were then subdivided into bins based on the radial distance, in the plane of the orbit of (3200) Phaethon, from the orbit of (3200) Phaethon. For each mean anomaly bin, the radial bin with the peak density was chosen to be representative of the stream. To create a continuous fit and to facilitate comparison with Battams et al. (2022), we then fit a parabola that took in mean anomaly as the independent variable and returned the radial offset from the orbit of (3200) Phaethon to these representative points. The coefficients of the fit equation  $y = ax^2 + bx + c$  for each model are given in Table 2.

We note that stream for the most part lies to the inside of the orbit of (3200) Phaethon, with the only exception being the Basic Model very close to perihelion. Additionally, none of the models are symmetric around perihelion, the streams of the Basic Model and the Violent Creation Model are both to first order further from the Sun just after perihelion compared to just before perihelion while the Cometary Creation Model is the opposite. The Basic Model and Cometary Creation Model are concave down to second order meaning that the further from perihelion, the more interior the particles are, while the Violent Creation Model is instead concave up. Observations from PSP near the perihelion of (3200) Phaethon as reported by Battams et al. (2022) show that contrary to our Basic Model and Cometary Model, the stream is in large part outside the orbit of (3200) Phaethon and concave up to second order. These observations do, however, agree with our model in the asymmetry about perihelion. Overall, these observations

are most consistent with our Basic Model which is exterior to the orbit of (3200) Phaethon at perihelion and our Violent Creation Model which is concave up around perihelion.

### 3.3.2. DESTINY+

The JAXA/DESTINY+ mission is planned to rendezvous with (3200) Phaethon (Sarli et al. 2018). Onboard it carries the DESTINY+ Dust Analyzer (DDA), a dust detector capable of compositional determination of impacting dust grains with an effective area of  $350 \text{ cm}^2$  (Kobayashi et al. 2018). In addition to the direct observations of grains from Phaethon’s impact ejecta cloud (Szalay et al. 2019), DESTINY+ will make important observations of interplanetary and interstellar dust during its cruise phase (Kruger et al. 2019).

We simulated the passage of an orbit similar to DESTINY+ through the Geminids stream and found that although the rate of impacts might be detectable over the background level, the total expected detections throughout the mission of Geminids grains was less than 1 impact. Hence, we anticipate DESTINY+ will likely be moving too rapidly through the core of the stream to have any Geminids dust hit its dust analyzer.

## 4. DISCUSSION AND CONCLUSIONS

We have simulated the Geminids meteoroid stream using a number of models and analyzed the Geminids flux upon Earth, Parker Solar Probe, and DESTINY+. Comparing to remote imaging of the Geminids stream (Battams et al. 2022), we find the observed stream location external to the orbit of (3200) Phaethon is most consistent with a formation mechanism of a rapid low-speed release of material near perihelion, not by a more temporally extended cometary formation mechanism. Hence, this comparison suggests the Geminids may have formed via a more violent, catastrophic destruction of bodies that transit very near to the Sun (Granvik et al. 2016; MacLennan et al. 2021). This is also consistent with the cross-comparison of mass of the Geminids stream and mass of (3200) Phaethon (Blaauw 2017; Ryabova 2017), which are comparable and suggestive of a catastrophic origin. Similarly, the weaker Daytime Sextantids meteoroid stream, suggested to be part of the Geminid-Phaethon stream complex, has been estimated to also be comparably massive to its proposed parent body asteroid 2005 UD (Kipreos et al. 2022), also consistent with a catastrophic common origin for both streams.

Our models, however, fail to directly hit Earth or to replicate the exact timing of the Geminids shower—the peak flux at Earth is just less than 1.5 days after the observed peak for the models. This discrepancy which has been reported in other models of the Geminids stream needs more investigation to determine its source. We additionally report mass estimates in the range of  $6.3 \times 10^{13} \text{ g}$  to  $8.6 \times 10^{14} \text{ g}$  which are respectively slightly lower than and consistent with the low side other estimates in the literature (Ryabova 2017; Blaauw 2017).

It is important to note that our model assumed particles with an “asteroidal” composition defined by Wilck & Mann (1996) and bulk density  $\rho = 3205 \text{ kg/m}^3$ . Changes in the composition of the particles can change the  $\beta$ -values and thus drastically affect the weighting functions. Additionally, the prediction of meteoroid impacts was done by taking the density of a sphere on the order of a few hundredths of an AU, which is significantly larger than any of the detectors considered. The mass, timing, and duration of the stream at Earth are all sensitive to the choice of the radius of this sphere—we have tried to pick a value which is reasonable and still captures information about the stream locally while not losing too much data to small number statistics.

We find the Geminids stream is likely not observable via in-situ impact detections with the Parker Solar Probe, at least with realistic upper limits on the mass of the Geminids stream. We additionally have shown that the formation mechanism of the stream dramatically changes the final shape and width of the stream. By further observing stream morphology via direct imaging to resolve the spatial structure with PSP near perihelion or with other future missions, we likely would be able to significantly constrain formation mechanisms. We also have demonstrated some properties of the Geminids stream such as how Poynting-Robertson drag has led to a reduction in the semi-major axis of particles and segregates them based on size—lighter particles generally exist on the inside edge of the stream while heavier particles mostly exist on the outside edge of the stream with the extremely light particles creating a secondary stream exterior to the orbit of (3200) Phaethon.

An alternative explanation for the PSP post-perihelion impact rate enhancement is that it is the result of the collisional byproducts, a  $\beta$ -stream, from the Geminids as that was not modeled here and the proximity of PSP to the Geminids makes it still a possible candidate (Szalay et al. 2021). Future work can use images from the WISPR instrument on PSP (e.g. Battams et al. 2022) to compare with and refine our models of the Geminids stream. More modeling could be done to understand the dust impacts upon PSP, such as understanding if it would be possible to directly observe a meteoroid stream, or the Geminids stream in particular, by flying through its core. Additionally,

as the DESTINY+ mission is visiting (3200) Phaethon, data from that mission will likely help us understand the Geminids stream and other meteoroid streams in general.

Future observations that are able to measure asymmetries in the stream before and after perihelion and which compare the position of the stream to that of the orbit of (3200) Phaethon can likely constrain the formation mechanism further. Comparisons between the direct visual imaging of the Geminids by PSP (e.g. Battams et al. 2020, 2022), notably the location and the width of the stream at multiple locations, could be used to further constrain the origin and evolution of the Geminids, utilizing the stream as a valuable laboratory to investigate meteoroid stream formation and dynamics throughout the solar system.

#### SOFTWARE AVAILABILITY

All code used for this paper is available at [https://github.com/wcukier/Phaethon\\_Meteoroids](https://github.com/wcukier/Phaethon_Meteoroids)

#### ACKNOWLEDGEMENTS

We thank Petr Pokorný for helpful modeling discussions and Harald Krüger for discussions on the DESTINY+ trajectory. We acknowledge the Parker Solar Probe Guest Investigator Program, grant 80NSSC21K1764. WC would like to thank the Hewlett Foundation Fund and the Princeton Undergraduate Fund for Academic Conferences for funding relevant conference travel.

*Software:* Spiceypy (Annex et al. 2020), SPICE (Acton et al. 2018; Acton 1996), Rebound (Rein & Liu 2012), Reboundx (Tamayo et al. 2020), Matplotlib (Hunter 2007), Numpy (Harris et al. 2020), Scipy (Virtanen et al. 2020)

#### REFERENCES

- Acton, C., Bachman, N., Semenov, B., & Wright, E. 2018, 150, 9, doi: [10.1016/j.pss.2017.02.013](https://doi.org/10.1016/j.pss.2017.02.013)
- Acton, C. H. 1996, 44, 65, doi: [10.1016/0032-0633\(95\)00107-7](https://doi.org/10.1016/0032-0633(95)00107-7)
- Annex, A. M., Pearson, B., Seignovert, B., et al. 2020, 5, 2050, doi: [10.21105/joss.02050](https://doi.org/10.21105/joss.02050)
- Arlt, R., & Rendtel, J. 2006, Monthly Notices of the Royal Astronomical Society, 367, 1721
- Bale, S. D., Goetz, K., Harvey, P. R., et al. 2016, Space Science Reviews, 204, 49
- Battams, K., Knight, M. M., Kelley, M. S. P., et al. 2020, The Astrophysical Journal Supplement Series, 246, 0
- Battams, K., Gutarra-Leon, A. J., Gallagher, B. M., et al. 2022, The Astrophysical Journal, 936, 81, doi: [10.3847/1538-4357/ac83b5](https://doi.org/10.3847/1538-4357/ac83b5)
- Blaauw, R. C. 2017, Planetary and Space Science, 143, 83
- Brown, P., Weryk, R., Wong, D. K., & Jones, J. 2008, Icarus, 195, 317
- Burns, J. A., Lamy, P. L., & Soter, S. 1979, Icarus, 40, 1, doi: [10.1016/0019-1035\(79\)90050-2](https://doi.org/10.1016/0019-1035(79)90050-2)
- Durda, D. D. 1996, Icarus, 120, 212, doi: [10.1006/icar.1996.0046](https://doi.org/10.1006/icar.1996.0046)
- Folkner, W. M., Williams, J. G., Boggs, D. H., Park, R. S., & Kuchynka, P. 2014, 81
- Fox, K., Williams, I. P., & Hughes, D. W. 1982, Monthly Notices of the Royal Astronomical Society, 200, 313
- . 1983, Monthly Notices of the Royal Astronomical Society (ISSN 0035-8711), 205, 1155
- Fox, N., Velli, M. C., Bale, S. D., et al. 2016, Space Science Reviews, 204, 7
- Granvik, M., Morbidelli, A., Jedicke, R., et al. 2016, Nature, 530, 303
- Greg, R. P. 1872, MNRAS, 32, 345, doi: [10.1093/mnras/32.9.345](https://doi.org/10.1093/mnras/32.9.345)
- Hajduková Jr, M., Kolen, P., Kornoš, L., & Tóth, J. 2017, Planetary and Space Science, 143, 89
- Harris, C. R., Millman, K. J., van der Walt, S. J., et al. 2020, Nature, 585, 357, doi: [10.1038/s41586-020-2649-2](https://doi.org/10.1038/s41586-020-2649-2)
- Hunter, J. D. 2007, Computing in Science & Engineering, 9, 90, doi: [10.1109/MCSE.2007.55](https://doi.org/10.1109/MCSE.2007.55)
- Jakubík, M., & Neslušan, L. 2015, Monthly Notices of the Royal Astronomical Society, 453, 1186
- Jenniskens, P. 1994, Astronomy and Astrophysics 287, 287, 990
- Jewitt, D., & Hsieh, H. 2006, The Astronomical Journal, 132, 1624, doi: [10.1086/507483](https://doi.org/10.1086/507483)
- Jewitt, D., Mutchler, M., Agarwal, J., & Li, J. 2018, The Astronomical Journal, 156, 238, doi: [10.3847/1538-3881/aae51f](https://doi.org/10.3847/1538-3881/aae51f)
- Jewitt, D. C., & Li, J. 2010, The Astronomical Journal, 140, 1519, doi: [10.1088/0004-6256/140/5/1519](https://doi.org/10.1088/0004-6256/140/5/1519)
- Jewitt, D. C., Li, J., & Agarwal, J. 2013, The Astrophysical Journal Letters, 771, L36
- Jones, J., Brown, P., Ellis, K. J., et al. 2005, Planetary and Space Science, 53, 413, doi: [10.1016/j.pss.2004.11.002](https://doi.org/10.1016/j.pss.2004.11.002)

- Kero, J., Szasz, C., & Nakamura, T. 2013, *Annales Geophysicae*, 31, 439, doi: [10.5194/angeo-31-439-2013](https://doi.org/10.5194/angeo-31-439-2013)
- Kimura, H., Ohtsuka, K., Kikuchi, S., et al. 2022, *Icarus*, 382, 115022, doi: <https://doi.org/10.1016/j.icarus.2022.115022>
- King, A. 1926, *Monthly Notices of the Royal Astronomical Society*
- Kipreos, Y., Campbell-Brown, M., Brown, P., & Vida, D. 2022, *Monthly Notices of the Royal Astronomical Society*, 516, 924, doi: [10.1093/mnras/stac2249](https://doi.org/10.1093/mnras/stac2249)
- Kobayashi, M., Srama, R., Krüger, H., Arai, T., & Kimura, H. 2018, in *Lunar and Planetary Institute Science Conference Abstracts*, Vol. 49, 2050
- Kozai, Y. 1962, *AJ*, 67, 591, doi: [10.1086/108790](https://doi.org/10.1086/108790)
- Krüger, H., Strub, P., Sommer, M., et al. 2020, *Astronomy and Astrophysics*, 643, A96
- Kruger, H., Strub, P., Srama, R., et al. 2019, *Planetary and Space Science*, 172, 22
- Li, J., & Jewitt, D. C. 2013, *The Astronomical Journal*, 145, 154, doi: [10.1088/0004-6256/145/6/154](https://doi.org/10.1088/0004-6256/145/6/154)
- MacLennan, E., Toliou, A., & Granvik, M. 2021, *Icarus*, 366, 114535, doi: <https://doi.org/10.1016/j.icarus.2021.114535>
- Malaspina, D. M., Szalay, J. R., Pokorný, P., et al. 2020, *Observations of Inner Heliospheric Dust Variability*
- Mann, I., Kimura, H., Biesecker, D. A., et al. 2004, *Space Science Reviews*, 110, 269
- Neslušan, L. 2015, *Contributions of the Astronomical Observatory Skalnaté Pleso*, 45, 60
- Page, B., Bale, S. D., Bonnell, J. W., et al. 2020, *Examining Dust Directionality with the Parker Solar Probe FIELDS Instrument*
- Pusack, A., Malaspina, D. M., Szalay, J. R., et al. 2021, *PSJ*, 2, 186, doi: [10.3847/PSJ/ac0bb9](https://doi.org/10.3847/PSJ/ac0bb9)
- Rein, H., & Liu, S. F. 2012, *A&A*, 537, A128, doi: [10.1051/0004-6361/201118085](https://doi.org/10.1051/0004-6361/201118085)
- Rein, H., & Spiegel, D. S. 2015, *MNRAS*, 446, 1424, doi: [10.1093/mnras/stu2164](https://doi.org/10.1093/mnras/stu2164)
- Ryabova, G. 2017, *Planetary and Space Science*, doi: [http://dx.doi.org/10.1016/j.pss.2017.02.005](https://doi.org/10.1016/j.pss.2017.02.005)
- Ryabova, G. O. 1999, *Solar System Research*, 33, 224
- Ryabova, G. O. 2007, *Monthly Notices of the Royal Astronomical Society*, 375, 1371
- . 2008, *Earth, Moon, and Planets*, 102, 95
- Ryabova, G. O. 2016, *MNRAS*, 456, 78, doi: [10.1093/mnras/stv2626](https://doi.org/10.1093/mnras/stv2626)
- . 2021, *MNRAS*, 507, 4481, doi: [10.1093/mnras/stab2286](https://doi.org/10.1093/mnras/stab2286)
- Sarli, B. V., Horikawa, M., Yam, C. H., Kawakatsu, Y., & Yamamoto, T. 2018, *The Journal of the Astronautical Sciences*, 65, 82
- Szalay, J. R., Pokorný, P., Horányi, M., et al. 2019, *Planetary and Space Science*, 165, 194, doi: [10.1016/j.pss.2018.11.001](https://doi.org/10.1016/j.pss.2018.11.001)
- Szalay, J. R., Pokorný, P., Jenniskens, P., & Horányi, M. 2018, *Monthly Notices of the Royal Astronomical Society*, 474, 4225, doi: [10.1093/mnras/stx3007](https://doi.org/10.1093/mnras/stx3007)
- Szalay, J. R., Pokorný, P., Bale, S. D., et al. 2020, *The Astrophysical Journal Supplement Series*, 246, 27, doi: [10.3847/1538-4365/ab50c1](https://doi.org/10.3847/1538-4365/ab50c1)
- Szalay, J. R., Pokorný, P., Malaspina, D. M., et al. 2021, *PSJ*, 2, 185, doi: [10.3847/PSJ/abf928](https://doi.org/10.3847/PSJ/abf928)
- Tabeshian, M., Wiegert, P., Ye, Q., et al. 2019, *The Astronomical Journal*, 158, 30, doi: [10.3847/1538-3881/ab245d](https://doi.org/10.3847/1538-3881/ab245d)
- Tamayo, D., Rein, H., Shi, P., & Hernandez, D. M. 2020, *MNRAS*, 491, 2885, doi: [10.1093/mnras/stz2870](https://doi.org/10.1093/mnras/stz2870)
- Virtanen, P., Gommers, R., Oliphant, T. E., et al. 2020, *Nature Methods*, 17, 261, doi: [10.1038/s41592-019-0686-2](https://doi.org/10.1038/s41592-019-0686-2)
- Wilck, M., & Mann, I. 1996, *Planetary and Space Science*, 44, 493
- Williams, I. P., & Ryabova, G. O. 2011, *Monthly Notices of the Royal Astronomical Society*, 415, 3914
- Zigo, P., Porubcan, V., Cevolani, G., & Pupillo, G. 2009, *Contributions of the Astronomical Observatory Skalnaté Pleso*, 39, 5